88

PRACTICAL LIMITATIONS TO INDENTATION TESTING OF THIN FILMS.

J.A. Schneider, K.F. McCarty, J.R. Heffelfinger, and N.R. Moody
Sandia National Laboratories, Livermore, CA 94551

ABSTRACT

A method that is becoming increasingly common for measuring the mechanical behavior of thin films is low-load indentation testing. However, there can be complications in interpreting the results as many factors can affect hardness and moduli measurements such as surface roughness and determination of the indentation contact area. To further our understanding, the mechanical properties of thin (50 nm) films of AlN on sapphire substrates were evaluated using a scanning force microscopy (SFM) based pico-indentation device to allow imaging of the surface and indentations. Our primary emphasis was the types of problems or limitations involved in testing very thin, as deposited films in which properties are desired over indentation depths less than 50 nm.

INTRODUCTION

Understanding the structure of thin film coatings on substrates and its relationship to the mechanical properties is being recognized as a key to predicting the ultimate reliability of electronic devices that employ this structure. However, due to the small size and volume of these thin films, conventional methods to measure the mechanical properties cannot be used. Low-load indentation techniques, or nanoindentation, are currently being developed [1, 2] that use the stiffness of the thin film along with the contact area of the indentation to calculate elastic moduli and hardness. True determination of this contact area is often cited as a limitation in the method at very shallow indentation depths where different phenomena can affect the actual area such as the geometrical tip defect, pile-up or sink-in around the indentation and the local roughness of the surface [3, 4]. Recent improvements with devices [4] that provide in-situ imaging of surfaces via SFM before and after indentations provide a method for obtaining information on the nature of very shallow (< 50 nm) indentations.

EXPERIMENTAL WORK

The hardness and elastic moduli of AlN were determined from indentations made using two commercially available low load indenters, a Nanoindenter II ™ and a Hysitron TriboScope® attachment on a NanoScope II (SFM). A triangular (Berkovich) pyramid-shape diamond indenter tip was used on both indenters. Indentation loads and corresponding depths are continuously recorded throughout each test. A contact area function was determined from calibration curves of indentations into a known modulus material for each indenter tip. Use of this contact area function and the recorded depth of the indenter allow calculation of the elastic moduli and hardness properties using the method of Oliver and Pharr [2].

AlN films were deposited on actively heated sapphire (0001) substrates by molecular beam epitaxy (MBE). Substrates were cleaned in solvents and mild hydrochloric acid, rinsed in de-ionized water, and blown dry with nitrogen. In the ultrahigh vacuum chamber, the substrates were heated to about 700° C, cooled, and examined by low energy electron diffraction (LEED) and Auger spectroscopy to verify the crystallinity and cleanliness of the surface, respectively. After heating to the deposition temperature, the substrates were exposed to an aluminum flux from an effusion cell and a nitrogen atom flux from a commercial source consisting of a radio frequency plasma discharge and an aperture. The AlN films were confirmed to be epitaxial by post growth examination by LEED. Film thickness was estimated by a stylus profilometer.

RESULTS AND DISCUSSION

Microstructure

Evidence of epitaxy is shown in the transmission electron microscopy (TEM) analysis of a 110 nm thick AlN film deposited on 700° C sapphire substrate shown in Figure 1. The corresponding selected area diffraction (SAD) pattern in Figure 2, was taken along the coincident [0001] zones of AlN and Al_2O_3 and shows the alignment of the film and the substrate. The (0001) plane of AlN is parallel to the (0001) plane of Al_2O_3 and the $[11\bar{2}\,0]$ direction in AlN parallel to the $[10\bar{1}\,0]$ direction in Al_2O_3. A Moiré pattern arises in the bright field image in Figure 2 due to the coincidence of the $(10\bar{1}\,0)$ AlN reflection with the $(11\bar{2}\,0)$ Al_2O_3 reflection. Similar microstructures were noted in films grown on 900° C substrates.

The well aligned grains have a rough, granular surface when examined in the SEM and also using the SFM capability of the Hysitron. Mechanical properties were evaluated for two AlN films grown at substrate temperatures of 700° and 900° C. Surface profiles are shown in Figure 3 comparing the two films with an approximate image of the Berkovich tip superimposed over the surfaces. For the 700° C film, with a peak-valley roughness of 15 nm, the tip is likely to hit either peaks or valleys. For the 900° C film, with a peak-valley roughness of 30 nm, in addition to the tip hitting either peaks or valleys, it may also occur on a intermediate point.

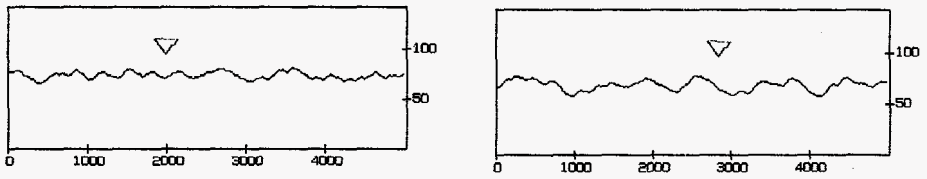

Figure 3. Profile of surface Roughness of AlN films grown on (a) 700° C and (b) 900° C sapphire substrates using Hysitron/NanoScope II with cubic diamond tip. Profiles are shown plotted in nm's.

Elastic Moduli and Hardness

The method used to calculate elastic modulus and hardness [2] utilizes the load and displacement data taken as the indentation is made (Figure 4). Hardness, H, (eqn. 1) is calculated from the peak load, P_{max} over the contact area, A_c . The reduced elastic modulus, E, (eqn. 2) is determined from the slope of the unloading curve (stiffness, S) divided by the square root of the contact area, A_c. The effects of the indenter can be subtracted to give the elastic modulus of the specimen, E_s (eqn. 3). All data can be extracted from the unloading curve, except for the contact area. This area is deduced from the contact depth extrapolated from the initial portion of the unloading curve.

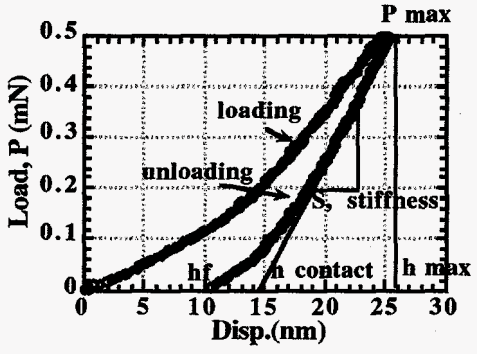

$$H = \frac{P_{Max}}{A_c} \qquad (1)$$

$$E_r = \frac{S\sqrt{\pi}}{2\sqrt{A_c}} \qquad (2)$$

$$\frac{1}{E_r} = \left(\frac{1-\nu}{E}\right)_s + \left(\frac{1-\nu}{E}\right)_I \qquad (3)$$

Figure 4. Continuous indentation load (P) vs. displacement data (h).

The relationship between the contact depth and the area of contact is obtained by a series of indentations in a known modulus material such as fused silica. Indentations are made to various displacements over a range of interest with an area term calculated based on a constant modulus assumption. The plot of displacement and the area term are plotted as shown in Figure 5A and curve fit to a standard area function (eqn. 4), where c is a constant.

$$A_c = 24.5h_c^2 + c_1h_c + c_2h_c^{0.5} + c_3h_c^{0.25} + c_4h_c^{0.125} + c_5h_c^{0.0625} + c_6h_c^{0.03125} + c_7h_c^{0.015625} + c_8h_c^{0.0078125} \quad (4)$$

The first term of the standard area function describes the perfect shape of the indenter, the other terms describe deviations from the Berkovich geometry due to blunting of the tip. This provides a reasonably good fit over a fairly wide range of displacements (0-100 nm). However, for indentations less than 50 nm, this standard area fit overestimates the area (Figure 5B). A simple second order polynomial equation (eqn. 5) provides a better fit of the data over this lower region.

$$A_c = c_1 + c_2h_c + c_3h_c^2 \quad (5)$$

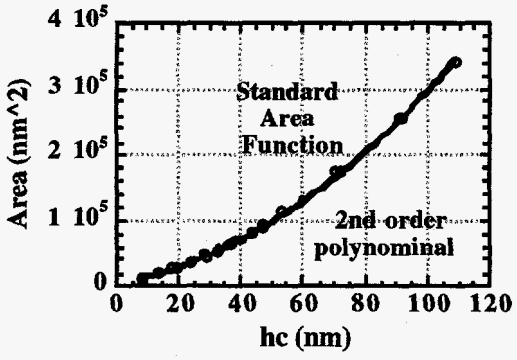

Figure 5A. Curve fitting of area function over wide range (0 to 100 nm) using standard area function vs. a 2nd order polynomial curve fit.

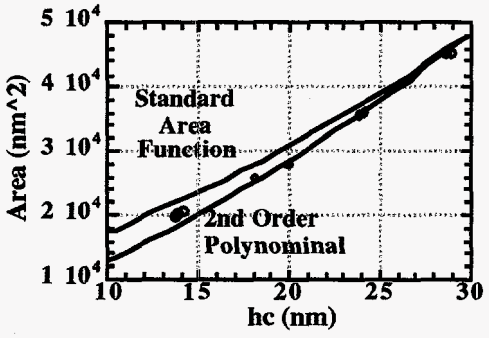

Figure 5B. Standard area function overestimates area at shallow indentations (< 30 nm).

Figure 6A is a plot of the reduced data from the Nanoindenter II using the polynomial area fit. This indenter is set up to do many series of indentations, in this case, 50 microns apart. The elastic modulus shown plotted versus indenter displacement indicates a slightly higher modulus for the film grown at 700 vs that at 900° C. These values converge as the indenter is pushed deeper into the substrate to values approaching sapphire. A similar trend is noted in the hardness shown plotted in Figure 6B. The 700° C film appears harder than the 900° C film initially before converging toward a value between sapphire and AlN.

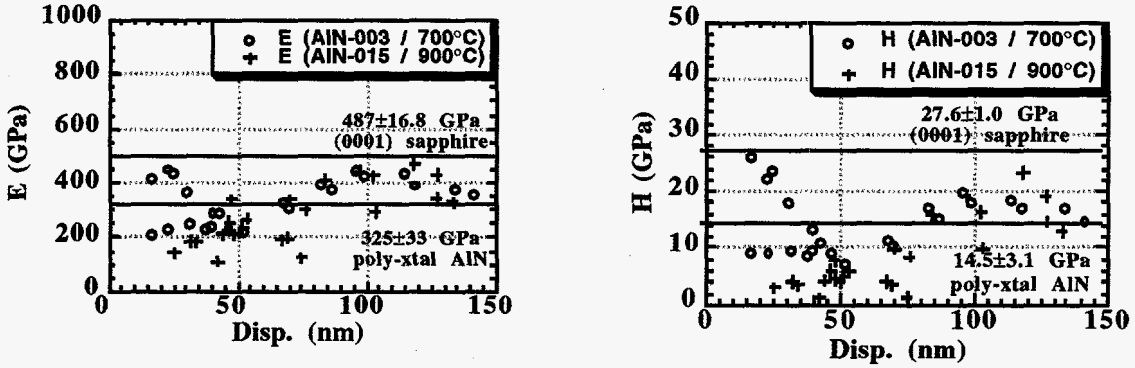

Figure 6. Properties of 50 nm thick AlN films obtained using Nanoindenter II (a) elastic modulus and (b) hardness. Horizontal lines indicate the properties of bulk (0001) sapphire and poly-xtal AlN.

Similar trends are also noted in data taken with the Hysitron. The only difference is now the areas are first scanned to find relatively flat portions to indent into. Again the elastic modulus and hardness of the 700° C film appear to be greater than that of the 900° C film as shown in the data in Figure 7A and 7B, respectively.

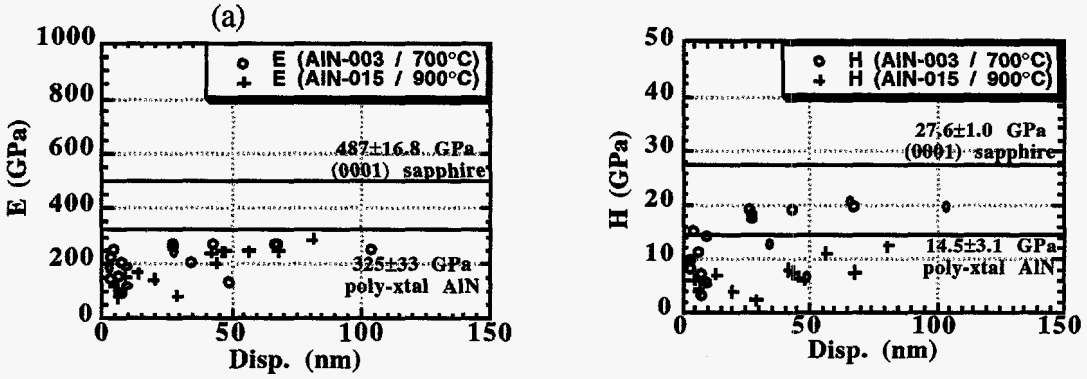

Figure 7. Properties of 50 nm thick AlN films obtained using Hysitron (a) elastic modulus and (b) hardness. Horizontal lines indicate the properties of bulk (0001) sapphire and poly-xtal AlN.

Table I lists the averaged data taken over the first 50 nm of indenter depth, corresponding to the film thickness, and shows fairly good agreement between the two instruments. Both indicate a higher elastic modulus (200-300 GPa) for the 700° C film compared with 150-200 nm for the 900° C film. These values, on the higher end, are close to that expected for bulk, polycrystalline AlN of 325 GPa. Similarly the hardness indicated by both devices is 12-14 GPa for the 700° C film compared to 4-5 for the 900° C film. The hardness of the 700° C film agrees favorably with that of bulk AlN at 14.5 GPa.

Table I. Comparison of Mechanical Properties of 50 nm thick AlN films on sapphire

	AlN-003	700° C	AlN-015	900° C
	NanoIndenter	Hysitron	NanoIndenter	Hysitron
E (GPa)	303±96	198± 58	201± 62	147 ± 62
H (GPa)	14 ± 6	12 ± 5	4 ± 2	5 ± 2

Images of typical indentations made by a 2 mN load are shown in Figure 8. The indentation in the 700° C film leaves an equal sided triangular pattern. Whereas in the 900° C film leaves a more irregular pattern, likely due to uneven striking of the surface with the indenter tip. Thus, for the 900° C film, the contact depth used to determine contact area would overpredict the actual contact area resulting in lower apparent properties. Use of direct measurements from the SFM image results in an overprediction of the projected area of the indentation due to the strong influence of blunting of the tip at very shallow indentations of 15-20 nm, similar to that seen by Pethica, et. al. [4].

SUMMARY

Nanoindentation techniques were used to measure the mechanical properties of as deposited 50 nm AlN films on sapphire substrates. Reasonable moduli and hardness values were obtained for the film grown at 700° C, due to a smoother surface. Direct SFM imaging of the indentations indicates the lower values at 900° C are due to the surface roughness. As indentations are made in very thin films, the contact area becomes extremely critical. Curve fitting with a second order polynomial may provide a better fit than that of the area function data for indentations less than 100 nm. Use of the standard area function leads to significant error over this range.

ACKNOWLEDGMENTS

The authors gratefully acknowledge the support of the U.S. Department of Energy under Contract #DE-AC04-94AL85000.

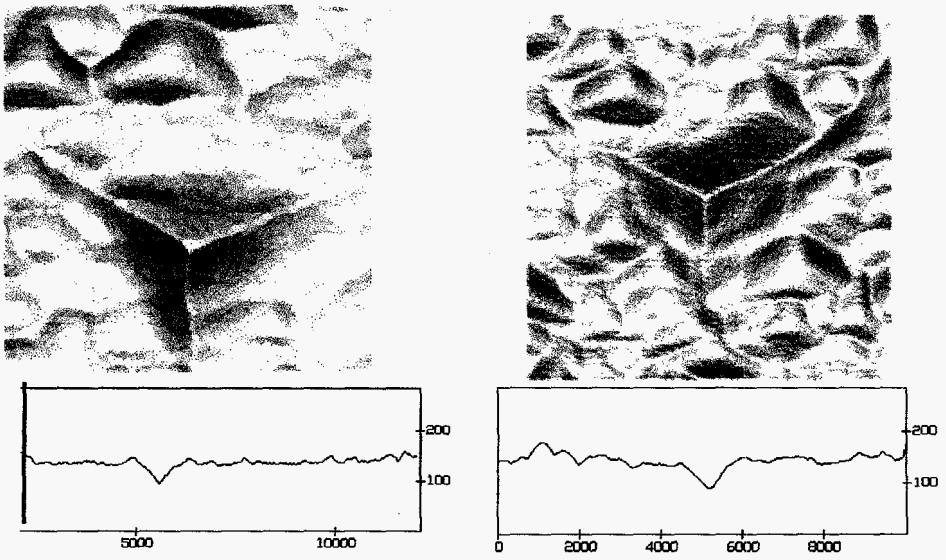

(a) (b)

Figure 8. Hysitron/Nanoscope II SFM images and surface profiles of indentations made at 2 mN load for AlN film grown on (a) 700° C and (b) 900° C sapphire substrates. Profiles are shown plotted in nm's.

REFERENCES

1) M.F. Doerner, W.D. Nix, "A method for interpreting the data from depth-sensing indentation instruments," *J. Mater. Res.*, **1**, [4], 601 (1986).

2) W.C. Oliver, G.M. Pharr, "An improved technique for determining hardness and elastic modulus using load and displacement sensing indentation experiments," *J. Mater. Res.*, **7**, [6], 1564 (1992).

3) J.B. Pethica, R. Hutchings, W.C. Oliver, "Hardness measurement at penetration depths as small as 20 nm," *Phil. Mag.*, **48A**, [4], 593 (1983).

4) B. Bhushan, S.V. Kulkarni, W. Bonin, J.T. Wyrobek, "Nanoindentation and picoindentation measurements using a capacitive transducer system in atomic force microscopy," *Phil. Mag.*, **74A**, [5], 1117 (1996).